Design of IIR lowpass differentiators using parallel allpass structure

Ivan Krstić[1*], Marijana Gavrilović Božović[1†], Goran Stančić[2†], Ivana Kostić[2†]

[1*]Department of Electrical Engineering, Faculty of Engineering, University of Kragujevac, Sestre Janjić 6, 34000 Kragujevac, Serbia.
[2]Department of Electronics, Faculty of Electronic Engineering, University of Niš, Aleksandra Medvedeva 14, 18000 Niš, Serbia.

*Corresponding author(s). E-mail(s): ivan.krstic@kg.ac.rs;
Contributing authors: marijana.gavrilovic@kg.ac.rs; goran.stancic@elfak.ni.ac.rs; ivana.kostic@elfak.ni.ac.rs;
†These authors contributed equally to this work.

Abstract

In this paper, design of infinite impulse response lowpass differentiators that can be realized by parallel connection of two allpass filters whose orders differ by two, where one of the allpass branches is pure delay, is considered. As adopted structure of proposed lowpass differentiators allows formulation of their magnitude and phase responses as functions of allpass filter phase response, a set of nonlinear equations in unknown allpass filter coefficients is derived and iteratively solved in a way that magnitude response approximates the ideal one in weighted Chebyshev sense, both in passband and stopband. On the other hand, passband phase response linearity is shown to be related to the maximum of the magnitude response, which can be directly controlled by an additional design parameter. Design examples reveal that proposed infinite impulse response lowpass differentiators of low order can have very low relative passband magnitude errors and nearly-linear phases, while results of comparison with existing lowpass differentiators show that proposed differentiators usually require fewer multiplications.

Keywords: digital lowpass differentiator, parallel allpass structure, digital allpass filter, nearly-linear phase, relative magnitude response error minimization

1 Introduction

High frequency noise filtering along with differentiation at low frequencies is required in various practical applications, among which are physiological signal processing [7, 11, 13, 19], extraction of velocity and acceleration data [16], edge-detection in image processing [6], and frequency estimation [14]. The frequency response of an ideal IIR lowpass differentiator having nonzero transition region width can be formulated as

$$\widetilde{H}\left(e^{j\omega}\right) = \begin{cases} j\omega e^{-j\omega\tau}, & \omega \leq \omega_p \\ 0, & \omega \geq \omega_s \end{cases}, \tag{1}$$

where τ is the passband group delay, while ω_p and ω_s are passband and stopband edge frequencies, respectively, and it can be approximated by the frequency response of either finite or infinite impulse response (IIR) filter. While a perfectly linear phase cannot be obtained by IIR filter, IIR lowpass differentiators are preferred over finite impulse response ones in applications where some amount of passband phase response nonlinearity can be tolerated, due to significantly lower filter order and lower group delay.

The majority of the IIR lowpass differentiators design methods belong to one of the following four approaches. The conventional approach is to cascade IIR fullband differentiator with the low-order lowpass filter [5, 17], while inversion-based design methods [2, 4, 10] start from the transfer function of IIR lowpass integrator, which is then inverted and stabilized by reflecting the unstable poles inside the unit circle. Methods of the third approach, i.e. the optimal methods [1, 5, 9, 12, 16, 18, 21], formulate the IIR lowpass differentiator design problem of simultaneous minimization of magnitude and phase response as the minimization problem in unknown filter coefficients. In [1, 5, 16], the numerator of the lowpass differentiator is assumed to be the linear phase filter, while denominator coefficients are determined using classical [5] and metaheuristic [1, 16] optimization methods. Method presented in [21] formulates the design problem in quadratic form without frequency sampling, while the method presented in [12] minimizes the group-delay deviation with respect to the average group delay under the constraints that the maximum relative passband magnitude error and average squared stopband magnitude response are below prescribed values. Another two optimal methods are presented in [9, 18], where lowpass differentiators based on parallel allpass structure are proposed. Finally, as the maximum-flatness-based methods provide the lowest approximation error at frequencies about some center frequency, methods of the fourth approach [9, 20, 22] consider design of the maximally flat IIR lowpass differentiators.

The assumption, recently introduced by authors in [18], that IIR lowpass differentiator can be realized by parallel connection of two allpass filters of the same order, with a pure delay in one of the allpass branches, has led to the development of a method for design of even-order nearly-linear phase allpass-based IIR lowpass differentiators that usually require fewer multiplications compared to differentiators obtained by other design approaches. An additional allpass structure, introduced in [9], suggests that lowpass differentiation can be performed by subtracting the output of the second-order allpass filter from the input signal, i.e. that the design problem of second-order IIR lowpass differentiator can be reduced to the design of the allpass filter of the same order. As discussed in [9], differentiators obtained in such a way are superior to the second-order differentiators from [18] in every aspect except the phase response linearity.

The novelty of this study is generalization of the equiripple design method discussed in [9] to an arbitrary order of the lowpass differentiator that can be realized by parallel connection of two allpass filters whose orders differ by two, where allpass branch of the lower order is a pure delay. This structure allows formulation of the differentiator magnitude and phase responses as functions of the corresponding allpass filter phase response and the value of an additional design parameter, which enables simultaneous minimization of both magnitude and phase response errors. Additionally, aforementioned generalization provides a means of controlling the stopband behavior of lowpass differentiators as the stopband edge frequency becomes one of the design parameters.

The rest of the paper is structured as follows. The problem formulation of the allpass-based nearly-linear phase IIR lowpass differentiator with magnitude response approximating the ideal one in weighted Chebyshev sense both in passband and stopband is discussed in Sec. 2. Proposed design method is presented in Sec. 3, while design examples and comparison with the existing lowpass differentiators are given in Sec. 4. Finally, conclusions are drawn in Sec. 5.

2 Problem formulation

Transfer function of the IIR lowpass differentiators considered in this paper is assumed to be of the following form

$$H(z) = \frac{\gamma}{2}\left(z^{-(L-2)} - A(z)\right), \quad \gamma > 0, \tag{2}$$

as depicted in Figure 1, where γ is the maximum of the magnitude response, while $A(z)$ is the Lth order transfer function of the stable allpass filter having distinct poles

$$A(z) = z^{-L}\frac{1+\sum_{i=1}^{L} a_i z^{i}}{1+\sum_{i=1}^{L} a_i z^{-i}}, \tag{3}$$

whose phase response is denoted by

$$\phi(\omega) = \arg\left\{A\left(e^{j\omega}\right)\right\} = -L\omega + 2\arctan\frac{\sum_{i=1}^{L} a_i \sin(i\omega)}{1+\sum_{i=1}^{L} a_i \cos(i\omega)}. \tag{4}$$

Substituting $z = e^{j\omega}$ in (2), phase and magnitude response of the considered IIR lowpass differentiators can be formulated as functions of the corresponding allpass

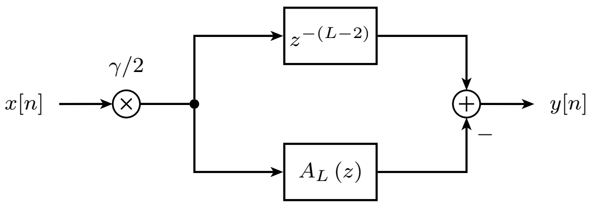

Fig. 1 Proposed realization structure of the IIR lowpass differentiator.

filter's phase response $\phi(\omega) = \arg\left\{A\left(e^{j\omega}\right)\right\}$ as follows

$$\varphi(\omega) = \arg\left\{H\left(e^{j\omega}\right)\right\} = \frac{\phi(\omega) - (L-2)\,\omega + \pi}{2}, \tag{5}$$

$$\left|H\left(e^{j\omega}\right)\right| = \gamma \left|\sin\frac{\phi(\omega) + (L-2)\,\omega}{2}\right|. \tag{6}$$

Now, since the phase response of the stable allpass filter $A(z)$ is monotonically decreasing function satisfying $\phi(0) = 0$ and $\phi(\pi) = -L\pi$ [15], from (5) and (6) it follows that $\varphi(0) = \pi/2$ and $\left|H\left(e^{j0}\right)\right| = \left|H\left(e^{j\pi}\right)\right| = 0$, i.e. the frequency response of the proposed IIR lowpass differentiators matches the ideal one at $\omega = 0$ and $\omega = \pi$, note (1). Additionally, as $\phi(\omega) + (L-2)\,\omega$ equals 0 at $\omega = 0$ and -2π at $\omega = \pi$, there exists frequency point ω^*, $0 < \omega^* < \pi$, where $\phi(\omega^*) + (L-2)\,\omega^* = -\pi$, that is where maximum of the magnitude response occurs, $\left|H\left(e^{j\omega^*}\right)\right| = \gamma$.

For the magnitude response of the proposed IIR lowpass differentiators given by (6) to approximate the ideal one,

$$\left|\widetilde{H}\left(e^{j\omega}\right)\right| = \begin{cases} \omega, \ \omega \le \omega_p \\ 0, \ \omega \ge \omega_s \end{cases}, \tag{7}$$

note (1), the phase response $\phi(\omega)$ of the allpass filter $A(z)$ should approximate either $\widetilde{\phi}_1(\omega)$ or $\widetilde{\phi}_2(\omega)$ defined as

$$\widetilde{\phi}_{1,2}(\omega) = \begin{cases} -(L-2)\,\omega \mp 2\arcsin\dfrac{\omega}{\gamma}, & \omega \le \omega_p \\ -(L-2)\,\omega - 2\pi, & \omega \ge \omega_s \end{cases}, \tag{8}$$

where parameter γ obviously needs to satisfy $\gamma \ge \omega_p$. Note that $\widetilde{\phi}_1(\omega)$ is monotonically decreasing regardless the value of the parameter γ for $\omega \in (0, \pi)$, while $\widetilde{\phi}_2(\omega)$ can be made so by a suitable choice of the parameter γ for $L > 2$.

In this paper, an iterative algorithm for the determination of the allpass filter $A(z)$ coefficients vector

$$\boldsymbol{a} = \left[a_1 \ a_2 \ \ldots \ a_L\right]^T, \tag{9}$$

for the predetermined value of the parameter γ is derived, such that the magnitude response of the obtained IIR lowpass differentiator approximates the ideal one in the weighted Chebyshev sense both in passband and stopband, i.e. such that the magnitude response error function

$$\varepsilon(\omega,\, \boldsymbol{a}) = W(\omega)\left(\left|H\left(e^{j\omega},\, \boldsymbol{a}\right)\right| - \left|\widetilde{H}\left(e^{j\omega}\right)\right|\right), \tag{10}$$

satisfies

$$\left|\varepsilon\left(\widehat{\omega}_k,\, \boldsymbol{a}\right)\right| = \delta_p, \tag{11}$$

for $k = 1,\, 2,\, \ldots,\, m$, and

$$\varepsilon\left(\overline{\omega}_k,\, \boldsymbol{a}\right) = \delta_s, \tag{12}$$

for $k = 1,\, 2,\, \ldots,\, L - m + 2$, where

$$W(\omega) = \begin{cases} 1/\omega, & \omega \le \omega_p \\ 1, & \omega \ge \omega_s \end{cases} \tag{13}$$

is weighting function that allows simultaneous minimization of the relative passband and absolute stopband magnitude response errors, $\delta_p = \max\limits_{\omega \le \omega_p} |\varepsilon(\omega,\, \boldsymbol{a})|$ and $\delta_s = \max\limits_{\omega \ge \omega_s} \varepsilon(\omega,\, \boldsymbol{a})$ are passband and stopband weighted Chebyshev norms, respectively, $m \le L + 1$ is the number of sign-alternating extrema in passband. Frequencies at which sign-alternating extremal values of $\varepsilon(\omega)$ occur in passband and stopband are $\widehat{\boldsymbol{\omega}} = \left[\widehat{\omega}_1\ \widehat{\omega}_2\ \ldots\ \widehat{\omega}_m\right]$ and $\overline{\boldsymbol{\omega}} = \left[\overline{\omega}_1\ \overline{\omega}_2\ \ldots\ \overline{\omega}_{L-m+2}\right]$, respectively, while $0 \le \widehat{\omega}_1 < \widehat{\omega}_2 < \cdots < \widehat{\omega}_m \le \omega_p$ and $\omega_s \le \overline{\omega}_1 < \overline{\omega}_2 < \cdots < \overline{\omega}_{L-m+2} < \pi$. Regarding the choice of the weighting function, note that lowpass differentiators are usually designed with constant relative passband magnitude response error [9, 12].

Since the relative passband magnitude error of the lowpass differentiators is being minimized, to circumvent the magnitude response error function given by (10) to be indeterminate for $\omega = 0$, sine term of the magnitude response is rewritten as

$$\begin{aligned} \sin\frac{\phi(\omega,\, \boldsymbol{a}) + (L-2)\,\omega}{2} &= \omega\lambda(\omega,\, \boldsymbol{a}) \\ &= \omega\frac{-\operatorname{sinc}\omega + \sum_{n=2}^{L}(n-1)\, a_n \operatorname{sinc}(\omega(n-1))}{\sqrt{\left(1 + \sum_{n=1}^{L} a_n \cos(n\omega)\right)^2 + \left(\sum_{n=1}^{L} a_n \sin(n\omega)\right)^2}}, \end{aligned} \tag{14}$$

where

$$\operatorname{sinc} x = \begin{cases} 1, & x = 0 \\ \sin x / x, & x \ne 0 \end{cases}. \tag{15}$$

Note that the transfer function (2) of the proposed IIR lowpass differentiators requires at least $2L - 2$ delays and $L + 1$ or L multiplications depending on the value of the parameter γ. Namely, if γ is expressed as the sum of a few power-of-two terms, required number of multiplications reduces to L.

2.1 Passband phase response linearity error

If $\left|H\left(e^{j\omega}\right)\right| \approx \left|\widetilde{H}\left(e^{j\omega}\right)\right|$, the passband phase response of the IIR lowpass differentiator $\varphi\left(\omega\right)$, given by (5), approximates

$$\widetilde{\varphi}_{1,2}\left(\omega\right) = \frac{\widetilde{\phi}_{1,2}\left(\omega\right) - \left(L-2\right)\omega + \pi}{2} = \frac{\pi}{2} - \left(L-2\right)\omega \mp \arcsin\frac{\omega}{\gamma}, \tag{16}$$

which is nearly-linear function of frequency for $\gamma \gg \omega_p$. On the other hand, to avoid dynamic range problem, the value of the parameter γ should be chosen with great concern. Furthermore, as the maximum of magnitude response, occurring at the frequency $\omega^* \geq \omega_p$, equals γ, γ should be close to ω_p to avoid excessive gain in the transition region or stopband. Therefore, proposed allpass-based IIR lowpass differentiators, i.e. the ones that can be realized by the structure given in Figure 1, are not capable of providing very low passband phase response linearity errors without increasing the maximum of the magnitude response beyond ω_p.

To quantify the previous claim, let us determine the lower and upper margin functions of the passband phase response linearity function defined as [12, 18]

$$\zeta\left(\omega\right) = \varphi\left(\omega\right) - \left(\frac{\pi}{2} - \omega\overline{\tau}\right), \tag{17}$$

where $\overline{\tau}$ is the average passband group delay

$$\overline{\tau} = \frac{\varphi\left(0\right) - \varphi\left(\omega_p\right)}{\omega_p}, \tag{18}$$

when relative passband magnitude response error is lower than δ_p, i.e. when

$$-\arcsin\frac{\omega\left(1+\delta_p\right)}{\gamma} \leq \frac{\phi\left(\omega\right) + \left(L-2\right)\omega}{2} \leq -\arcsin\frac{\omega\left(1-\delta_p\right)}{\gamma}, \tag{19}$$

for $\omega \leq \omega_p$, note (10) and (24). Substituting (5) and (18) in (17), passband phase response linearity function becomes

$$\zeta\left(\omega\right) = \frac{\phi\left(\omega\right)}{2} - \frac{\omega}{\omega_p}\frac{\phi\left(\omega_p\right)}{2}, \tag{20}$$

while its upper and lower margin functions can be determined by means of (19) as

$$\mathcal{U}\left(y = \frac{\omega}{\omega_p}\right) = y\arcsin\frac{1+\delta_p}{x} - \arcsin\frac{y\left(1-\delta_p\right)}{x}, \tag{21}$$

$$\mathcal{L}\left(y\right) = y\arcsin\frac{1-\delta_p}{x} - \arcsin\frac{y\left(1+\delta_p\right)}{x}, \tag{22}$$

where $x = \gamma/\omega_p$. Plots of

$$f(x,\,\delta_p) = \frac{180}{\pi} \cdot \max_{y\le 1} \left\{ \left|\mathcal{L}(y,\,x,\,\delta_p)\right|,\, \left|\mathcal{U}(y,\,x,\,\delta_p)\right| \right\}, \tag{23}$$

for $\delta_p \in \{0,\,3\%,\,6\%,\,9\%\}$ and $(1+\delta_p) \le x \le 2$ are shown in Figure 2. Note that maximum passband phase response linearity error $\max\limits_{\omega\le\omega_p} |\zeta(\omega,\,\gamma,\,\delta_p)|$ is lower than $f(x,\delta_p)$, while notations $\zeta(\omega,\,\gamma,\,\delta_p)$, $\mathcal{L}(y,\,x,\,\delta_p)$ and $\mathcal{U}(y,\,x,\,\delta_p)$ are used to emphasize the dependence of $\zeta(\omega)$ on γ and δ_p, and $\mathcal{L}(y)$ and $\mathcal{U}(y)$ on $x = \gamma/\omega_p$ and δ_p. It can be observed from these plots that even in a limiting case, that is for $\delta_p = 0$, if the passband phase response error is to be lower than 1 degree, γ should be higher than $1.5\omega_p$. Furthermore, with increase of maximum relative passband magnitude response error required γ/ω_p ratio increases.

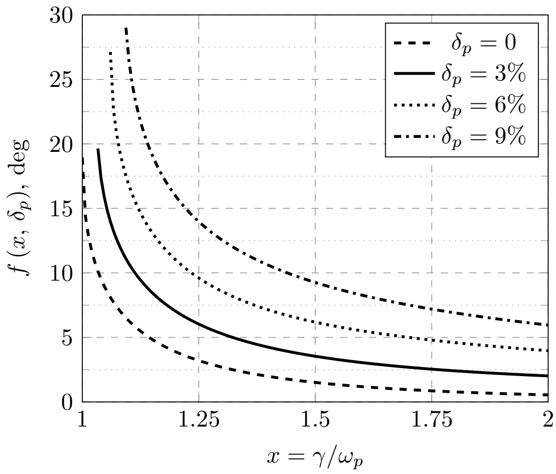

Fig. 2 Maximum absolute value of lower and upper margin functions for $\omega/\omega_p \le 1$ as a function of γ/ω_p for four values of δ_p.

3 Design method

Mathematical background of the proposed design method depends on whether $\phi(\omega,\,\boldsymbol{a})$ is assumed to approximate $\widetilde{\phi}_1(\omega)$ or $\widetilde{\phi}_2(\omega)$ given by (8). However, as $\widetilde{\phi}_2(\omega)$ is not monotonically decreasing function for every L and γ, it is adopted that $\phi(\omega,\,\boldsymbol{a})$ needs to approximate $\widetilde{\phi}_1(\omega)$. In this case, as $\widetilde{\phi}_1(\omega)$ is less than $-(L-2)\,\omega$ in passband, and reasonable assumptions that $\phi(\omega,\,\boldsymbol{a})$ is also less than $-(L-2)\,\omega$ in passband and that $\phi(\omega,\boldsymbol{a}) > -(L-2)\,\omega - 2\pi$ in the transition region are adopted, the magnitude response (6) of the proposed IIR lowpass differentiators can be rewritten as

$$\left|H\left(e^{j\omega},\,\boldsymbol{a}\right)\right| = -\gamma\omega\lambda(\omega,\,\boldsymbol{a}), \tag{24}$$

for $\omega \leq \omega_s$. Now, the magnitude response error function (10) at frequencies where its sign-alternating extremal values occur can be rewritten as

$$\varepsilon\left(\widehat{\omega}_k,\, \boldsymbol{a}\right) = -1 - \gamma\lambda\left(\widehat{\omega}_k,\, \boldsymbol{a}\right), \tag{25}$$

for $k = 1,\, 2,\, \ldots,\, m$, and

$$\varepsilon\left(\overline{\omega}_k,\, \boldsymbol{a}\right) = (-1)^{k+1}\, \overline{\omega}_k \gamma\lambda\left(\overline{\omega}_k,\, \boldsymbol{a}\right), \tag{26}$$

for $k = 1,\, 2,\, \ldots,\, L - m + 2$.

Therefore, (11) and (12), which characterize the proposed design method, can be rewritten by means of previous equations as

$$\lambda\left(\widehat{\omega}_k,\, \boldsymbol{a}\right) + (-1)^{p+k}\frac{\delta_p}{\gamma} = -\frac{1}{\gamma}, \quad k = 1,\, 2,\, \ldots,\, m, \tag{27}$$

$$\lambda\left(\overline{\omega}_k,\, \boldsymbol{a}\right) + (-1)^{k}\frac{\delta_s}{\gamma\overline{\omega}_k} = 0, \quad k = 1,\, 2,\, \ldots,\, L - m + 2, \tag{28}$$

where p determines whether the first extremal value of the passband magnitude response error function is maximum ($p = 1$) or minimum ($p = 0$). Evidently, a system of nonlinear equations given by (27) and (28) consists of $L + 2$ equations in $L + 2$ unknowns. It shows that it can be efficiently solved by following exchange algorithm:

1. Determine $\boldsymbol{a}'$ such that $\varepsilon\left(\omega,\, \boldsymbol{a}'\right)$ exhibits at least m and $L-m+2$ extremal values in the passband and stopband, respectively. As following relation can be established between the phase response and coefficients of the allpass filter $A_L\left(z\right)$,

$$\sum_{i=1}^{L} a_i \sin\frac{\phi\left(\omega\right) + \left(L - 2i\right)\omega}{2} = -\sin\frac{\phi\left(\omega\right) + L\omega}{2}, \tag{29}$$

   note (4), unknown coefficients vector $\boldsymbol{a}'$ can be determined as a solution to the system of linear equation obtained by setting $\phi\left(\omega\right) = \widetilde{\phi}_1\left(\omega\right)$ at $m-1$ and $L-m+1$ frequency points in passband and stopband, respectively,

$$\omega_k = \begin{cases} \left(k+2\right)\dfrac{\omega_p}{m+2}, & k < m \\ \omega_s + \left(k - m + 1\right)\dfrac{\pi - \omega_s}{L - m + 2}, & k \geq m \end{cases}, \tag{30}$$

   for $k = 1,\, 2,\, \ldots,\, L$.
2. Determine frequencies $\widehat{\boldsymbol{\omega}}' = \left[\widehat{\omega}_1' \; \widehat{\omega}_2' \; \ldots \; \widehat{\omega}_m'\right]$ and $\overline{\boldsymbol{\omega}}' = \left[\overline{\omega}_1' \; \overline{\omega}_2' \; \ldots \; \overline{\omega}_{L-m+2}'\right]$ where m and $L - m + 2$ sign-alternating extremal values of $\varepsilon\left(\omega,\, \boldsymbol{a}'\right)$ occur in passband and stopband, respectively. It was concluded empirically that $\varepsilon\left(\omega,\, \boldsymbol{a}'\right)$ can have one excess extremum in passband/stopband and that following heuristic approach can be used to select the required number of sign-alternating extremal values:

– if the first- or last-two extremal values in passband/stopband are of the same sign, then the first or last extrema is not taken into consideration, respectively.
– if there are $m+1$ sign-alternating extremal values in the passband, the lower between the first and last extrema is not taken into consideration for $\omega_p < \pi/2$, otherwise, the last extrema is not taken into consideration.
– if there are $L-m+2$ sign-alternating extremal values in the stopband, the lower between the first and last extrema is not taken into consideration.

3. Determine coefficients vector $\boldsymbol{a} = \boldsymbol{a}' + \Delta\boldsymbol{a}$ by solving the following system of linear equations

$$\begin{bmatrix} \widehat{\boldsymbol{\Psi}}(\boldsymbol{a}') & \gamma^{-1}\widehat{\boldsymbol{\eta}} & \mathbf{0}_{m\times 1} \\ \overline{\boldsymbol{\Psi}}(\boldsymbol{a}') & \mathbf{0}_{(L-m+2)\times 1} & \gamma^{-1}\overline{\boldsymbol{\eta}} \end{bmatrix} \begin{bmatrix} \Delta\boldsymbol{a} \\ \delta_p \\ \delta_s \end{bmatrix} = -\begin{bmatrix} \gamma^{-1}\cdot \mathbf{1}_{m\times 1} + \widehat{\boldsymbol{\lambda}}(\boldsymbol{a}') \\ \overline{\boldsymbol{\lambda}}(\boldsymbol{a}') \end{bmatrix}, \tag{31}$$

obtained by linearization of (27) and (28) about $\boldsymbol{a}'$ and adopting $\widehat{\boldsymbol{\omega}} = \widehat{\boldsymbol{\omega}}'$ and $\overline{\boldsymbol{\omega}} = \overline{\boldsymbol{\omega}}'$. In previous equation $\widehat{\boldsymbol{\Psi}}(\boldsymbol{a}') = \left[\widehat{\psi}_{ki}(\boldsymbol{a}')\right]$, $\overline{\boldsymbol{\Psi}}(\boldsymbol{a}') = \left[\overline{\psi}_{ki}(\boldsymbol{a}')\right]$, $\widehat{\boldsymbol{\lambda}}(\boldsymbol{a}') = \left[\widehat{\lambda}_k(\boldsymbol{a}')\right]$, $\overline{\boldsymbol{\lambda}}(\boldsymbol{a}') = \left[\overline{\lambda}_k(\boldsymbol{a}')\right]$, $\widehat{\boldsymbol{\eta}} = \left[\widehat{\eta}_k\right]$ and $\overline{\boldsymbol{\eta}} = \left[\overline{\eta}_k\right]$ are $m\times L$, $(L-m+2)\times L$, $m\times 1$, $(L-m+2)\times 1$, $m\times 1$ and $(L-m+2)\times 1$ matrices, respectively, with elements

$$\widehat{\psi}_{ki}(\boldsymbol{a}') = \frac{\partial\lambda\left(\widehat{\omega}_k', \boldsymbol{a}'\right)}{\partial a_i}, \quad \overline{\psi}_{ki}(\boldsymbol{a}') = \frac{\partial\lambda\left(\overline{\omega}_k', \boldsymbol{a}'\right)}{\partial a_i}, \tag{32}$$

$$\widehat{\lambda}_k(\boldsymbol{a}') = \lambda\left(\widehat{\omega}_k', \boldsymbol{a}'\right), \quad \overline{\lambda}_k(\boldsymbol{a}') = \lambda\left(\overline{\omega}_k', \boldsymbol{a}'\right), \tag{33}$$

$$\widehat{\eta}_k = (-1)^{p+k}, \quad \overline{\eta}_k = \frac{(-1)^k}{\overline{\omega}_k'}. \tag{34}$$

4. If $\max|\Delta\boldsymbol{a}| \le \Delta_{\mathrm{tol}}$, where $\Delta_{\mathrm{tol}} > 0$ is the prescribed tolerance, the algorithm converged to the solution. Otherwise, set $\boldsymbol{a}' \leftarrow \boldsymbol{a}$ and proceed to the step 2.

Note that since only the first m sign-alternating extremal values are considered for $\omega_p > \pi/2$, utilization of the proposed design method algorithm may not result in a valid transfer function (i.e. the one with relative magnitude response error at the passband edge higher than δ_p). The mentioned limitation will be considered in more detail in the following section.

4 Design examples and comparison with the existing IIR lowpass differentiators

In this section, examples of proposed allpass-based IIR lowpass differentiators are given and some conclusions regarding the impact of design parameters L, ω_p, ω_s, γ, and m on the passband phase response linearity and relative passband magnitude response errors are drawn. Δ_{tol} equals 10^{-10} in all examples. Additionally, a comparison with the existing allpass-based IIR lowpass differentiators from [18] and nearly-linear phase IIR lowpass differentiators from [5, 12] is presented. Here, it should be noted that second-order IIR lowpass differentiators obtained by the equiripple design method from [9] are the same ones obtained by the proposed design method for $L = 2$ and $m = 3$.

Various lowpass differentiators are compared in terms of the required number of multiplications and delay elements, maximum peak-to-peak passband phase response error in degrees

$$\eta = \frac{180}{\pi} \left[\max_{\omega \leq \omega_p} \zeta(\omega) - \min_{\omega \leq \omega_p} \zeta(\omega) \right], \tag{35}$$

average passband group delay

$$\overline{\tau} = \frac{L-2}{2} - \frac{\phi(\omega_p)}{2\omega_p}, \tag{36}$$

note (18), as well as values of $\delta_p = \max_{\omega \leq \omega_p} |\varepsilon(\omega, \boldsymbol{a})|$ and $\delta_s = \max_{\omega \geq \omega_s} \varepsilon(\omega, \boldsymbol{a})$. Additionally, average squared stopband magnitude response

$$P_{sb} = \frac{1}{\pi - \omega_p} \int_{\omega_p}^{\pi} \left| H\left(e^{j\omega}\right) \right|^2 \mathrm{d}\omega, \tag{37}$$

is used to properly characterize differentiators from [5, 12] in the stopband, as these differentiators do not consider stopband edge frequency as design parameter. Note that proposed allpass-based lowpass differentiators have $\min_{\omega \leq \omega_p} \zeta(\omega)$ equal to zero, as phase response of stable allpass filter is monotonically decreasing function of frequency, note (20).

In the first example, the proposed method is used to design IIR lowpass differentiators with lowest possible relative passband magnitude response error, i.e. the case when $m = L + 1$ is considered. As a case when $L = 2$ and $m = 3$ is discussed in [9], fourth-order IIR lowpass differentiators ($L = 3$) of various passband edges $\omega_p \in \{0.2\pi\,(1 + k/13) \mid 0 \leq k \leq 39\}$ and $\gamma/\omega_p \in \{1.02,\, 1.04,\, 1.06\}$ are considered here. Note that for $m = L + 1$ (31) reduces to

$$\begin{bmatrix} \widehat{\boldsymbol{\Psi}}(\boldsymbol{a}') & \gamma^{-1}\widehat{\boldsymbol{\eta}} \end{bmatrix} \begin{bmatrix} \Delta\boldsymbol{a} \\ \delta_p \end{bmatrix} = -\gamma^{-1} \cdot \mathbf{1}_{m\times 1} - \widehat{\boldsymbol{\lambda}}(\boldsymbol{a}'), \tag{38}$$

as stopband edge frequency is redundant parameter. Plots of δ_p, η and P_{sb} as functions of ω_p, for three values of γ/ω_p are shown in Figure 3. As can be observed from these plots, with the increase of the parameter γ, maximum relative passband magnitude response error δ_p and maximum passband phase response error η decrease, while average squared stopband magnitude response P_{sb} increases. δ_p is less than 0.86%, 0.65% and 0.51%, while η is less than 10.52 ($f\,(1.02,\, 0.86\%) = 14.72$), 8.93 ($f\,(1.04,\, 0.65\%) = 10.84$) and 7.76 ($f\,(1.06,\, 0.51\%) = 8.96$) degrees, for $0.2\pi \leq \omega_p \leq 0.8\pi$ and γ/ω_p equal to 1.02, 1.04, 1.06, respectively. As expected, the proposed fourth-order IIR lowpass differentiators have lower relative passband magnitude response error compared to the second-order lowpass differentiators [9].

In the second example, the proposed method is used to design sixth-order IIR lowpass differentiators of various passband edges $\omega_p \in \{0.2\pi\,(1 + 3k/59) \mid 0 \leq k \leq 59\}$,

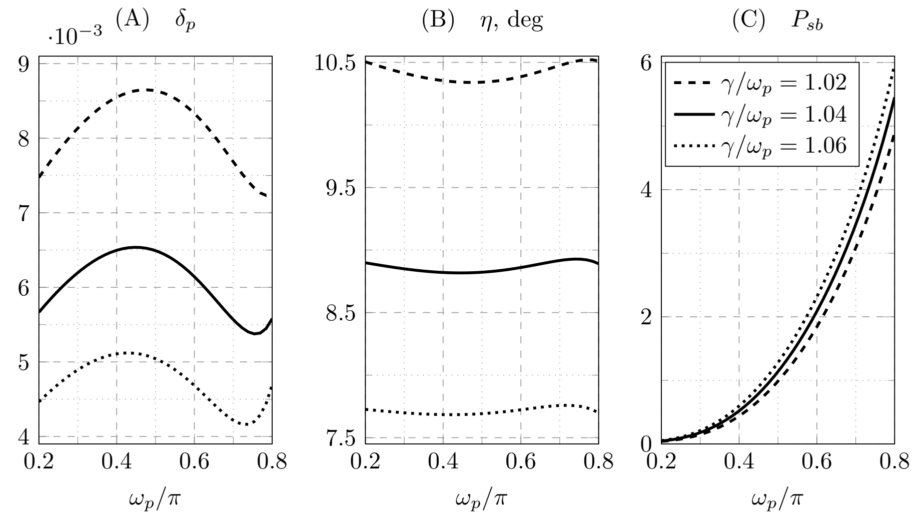

Fig. 3 Proposed fourth-order allpass-based IIR lowpass differentiators. (A) δ_p, (B) η and (C) P_{sb}, as functions of $\omega_p \in [0.2\pi,\, 0.8\pi]$ for three values of γ/ω_p and $L = 3$, $m = 4$.

$\omega_s = \omega_p + 0.18\pi$, $\gamma/\omega_p \in \{1.02,\, 1.04,\, 1.06\}$ and $m = L = 4$. Plots of δ_p, η and δ_s as functions of ω_p, for three values of γ/ω_p ratio are shown in Figure 4. Since only the first m sign-alternating extremal values are considered for $\omega_p > \pi/2$, utilization of the proposed design method does not result in a valid transfer function (i.e. the relative magnitude response at the passband edge is higher than δ_p obtained by the proposed algorithm) for $\omega_p > 0.7\pi$ ($\gamma/\omega_p = 1.02$), $\omega_p > 0.74\pi$ ($\gamma/\omega_p = 1.04$) and $\omega_p > 0.76\pi$ ($\gamma/\omega_p = 1.06$), $\omega_s = \omega_p + 0.18\pi$, $L = m = 4$. While parameters L, m and the transition region width $\omega_s - \omega_p$ also affect whether relative magnitude response error at the passband edge is higher than δ_p obtained by the algorithm, it is more probable to happen for ω_p closer to Nyquist frequency and γ/ω_p closer to one. From Figure 4 it can be also concluded that for $L \neq m + 1$, δ_p does not necessarily decrease when γ increases. On the other hand, when γ increases, η decreases, while δ_s increases.

In the third example, fourth-order allpass-based IIR lowpass differentiators of various stopband edges $\omega_s \in \{0.5\pi\,(1 + 0.6k/19) \,|\, 0 \leq k \leq 19\}$, $\omega_p = 0.4\pi$, $\gamma/\omega_p \in \{1.02,\, 1.04,\, 1.06\}$ and $m = L = 3$ are considered. Plots of δ_p, η and δ_s are shown in Figure 5. As expected, with the increase of the stopband edge frequency, δ_p, η and δ_s decrease.

Finally, in the fourth example, application of the proposed fourth-order lowpass differentiator with a real input - the electrooculogram (EOG) signal is tested, since its derivative is required for example to detect the direction of eye movements [11]. EOG signal is obtained from [8], and its sampling frequency equals 100Hz. Lowpass differentiator is designed using $\omega_p = 0.025\pi$, $\omega_s = 0.4\pi$, $L = m = 3$ and $\gamma = \omega_p$. Input and output signals of the lowpass differentiator are shown in Figure 6. Evidently, lowpass differentiation is required due to existence of high frequency noise in the input EOG signal.

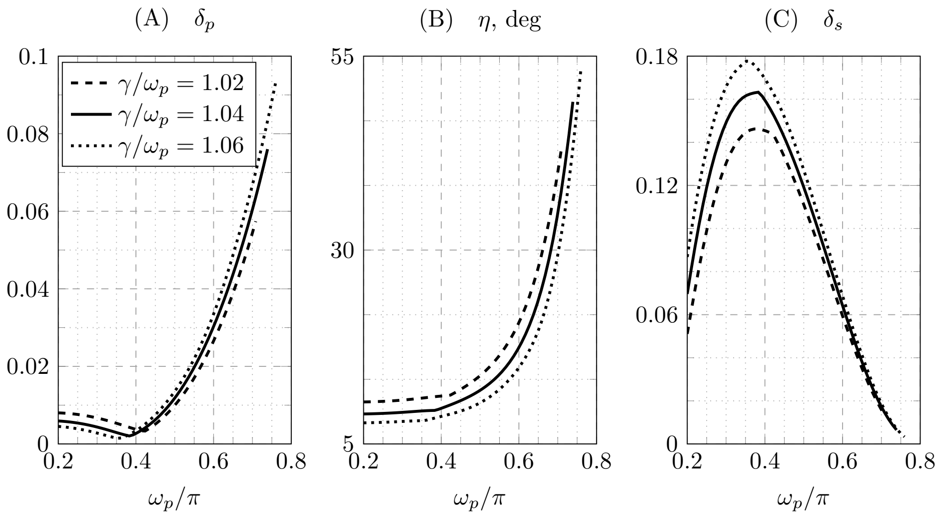

Fig. 4 $L = 4$, $m = 4$, $\omega_p \in [0.2\pi,\ 0.8\pi]$, $\omega_s = \omega_p + 0.18\pi$

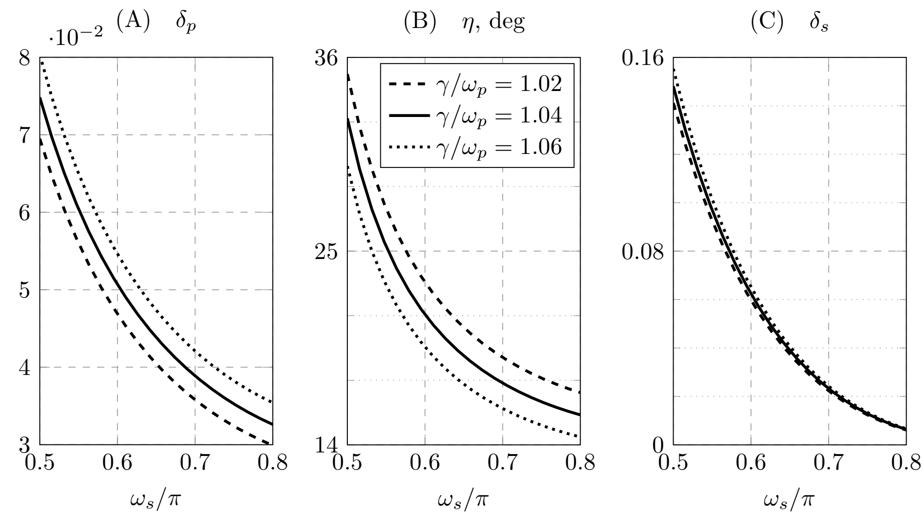

Fig. 5 $L = 3$, $m = 3$, $\omega_p = 0.4\pi$, $\omega_s \in [0.5\pi,\ 0.8\pi]$

4.1 Comparison with the allpass-based IIR lowpass differentiators from [18]

In this subsection, a comparison of the proposed nearly-linear phase allpass-based IIR lowpass differentiators with the ones from [18] is presented. These differentiators are also designed by minimizing the weighted Chebyshev norms both in the passband and the stopband, while their transfer function can be expressed as

$$H_1(z) = \frac{\gamma_1}{2}\left[A_1(z) - z^{-M}\right], \tag{39}$$

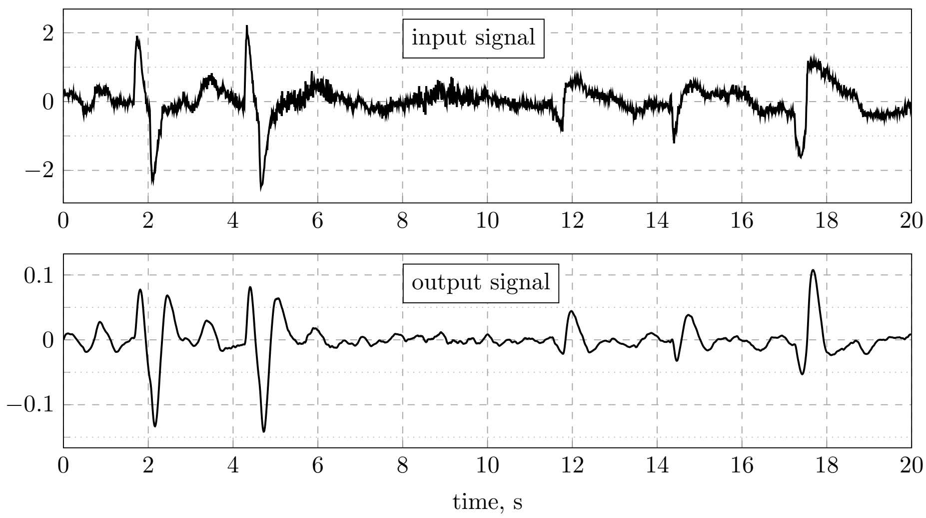

Fig. 6 EOG signal and output of the proposed fourth-order lowpass differentiator.

where $A_1(z)$ is the transfer function of Mth degree allpass filter.

In the fifth example, the proposed lowpass differentiators are compared to eighth-order ($M = 4$) differentiator from [18] with passband and stopband edge frequencies $\omega_p = 0.3\pi$ and $\omega_s = 0.57\pi$. Three competing differentiators are designed: a) $L = m = 3$, $\gamma = 1.118$, b) $L = m = 4$, $\gamma = 1.125$, and c) $L = 5$, $m = 4$, $\gamma = 2$. The results of comparison are presented in Table 1 and Figure 7. From these results, it can be observed that eighth-order lowpass differentiator designed using proposed method outperform the existing one of the same order from [18] in all terms except the required number of multiplications. On the other hand, proposed fourth and sixth-order differentiators have the same or smaller values of δ_p, δ_s and $\overline{\tau}$, while passband phase response errors of proposed differentiators are higher compared to differentiator from [18].

Table 1 $\omega_p = 0.3\pi$, $\omega_s = 0.57\pi$. Results of comparison of proposed differentiators with lowpass differentiator from [18].

Parameters	Proposed $L = m = 3$, $\gamma = 1.118$	Proposed $L = m = 4$, $\gamma = 1.125$	Proposed $L = 5$, $m = 4$, $\gamma = 2$	[18]
δ_p	2.41%	0.03%	0.33%	2.41%
δ_s	5.64%	11.35%	3.49%	11.94%
$\overline{\tau}$	2.10	3.05	3.52	3.6
η	6.62°	4°	0.49°	0.62°
no. of multiplications	4	4	5	4
no. of delays/filter order	4	6	8	8

In the sixth example, proposed lowpass differentiators are compared to the sixth-order ($M = 3$) lowpass differentiator from [18] with the passband and stopband edge

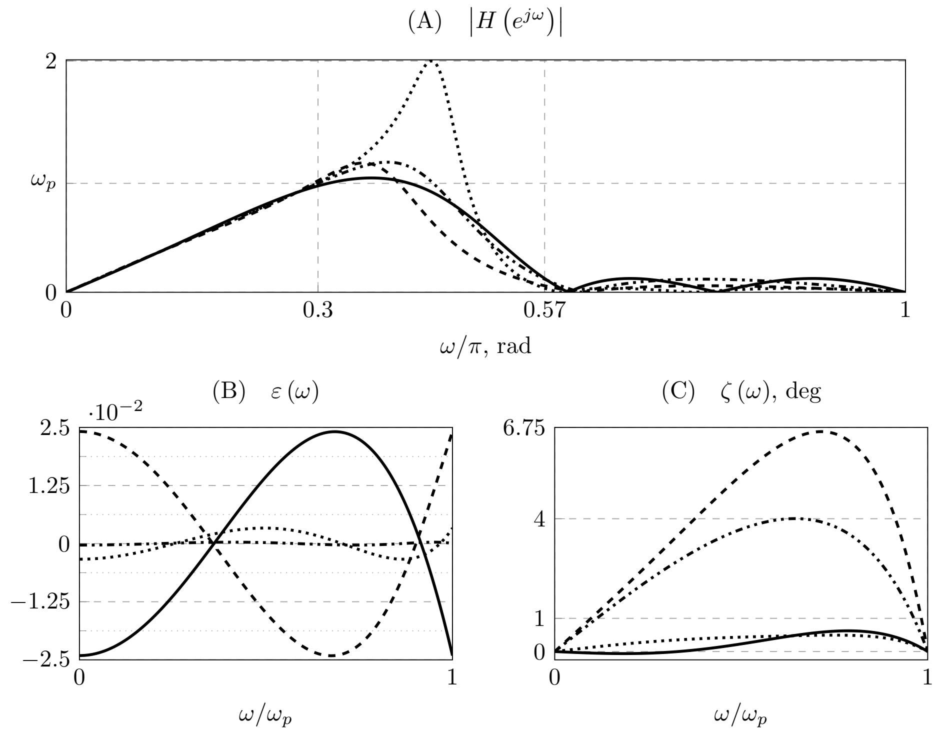

Fig. 7 $\omega_p = 0.3\pi$, $\omega_s = 0.57\pi$. (A) Magnitude responses, (B) relative passband magnitude response errors, and (C) passband phase response linearity errors of the IIR lowpass differentiator from [18] (solid line) and the proposed ones (dashed, dash dot dotted, dotted lines correspond to 4th, 6th and 8th order differentiators, respectively).

frequencies $\omega_p = 0.5\pi$ and $\omega_s = 0.725\pi$. Two competing differentiators of the sixth-order are designed: a) $L = m = 4$, $\gamma = 1.75$, and b) $L = m = 4$, $\gamma = 2.875$. The results of comparison are presented in Table 2. From these results it can be observed that both sixth-order lowpass differentiators designed using proposed method have much smaller maximum passband and stopband magnitude response errors, δ_p and δ_s, compared to existing differentiator of the same order from [18]. On the other hand, only lowpass differentiator having maximum passband magnitude equal to $\gamma = 2.875$ has smaller passband phase response error. In this example, both proposed differentiators require one multiplication more than existing differentiator of the same order.

In the seventh example, the proposed lowpass differentiators are compared to eighteenth-order ($M = 9$) lowpass differentiator from [18] with passband and stopband edge frequencies $\omega_p = 0.7\pi$ and $\omega_s = 0.825\pi$. Three competing differentiators are designed: a) $L = m = 6$, $\gamma = 2.25$, b) $L = m = 7$, $\gamma = 2.75$, and c) $L = 10$, $m = 9$, $\gamma = 2.75$. The results of comparison are presented in Table 3. From these results it can be concluded that eighteenth lowpass differentiator designed using the proposed method outperforms existing differentiator from [18] of the same order in all terms except the required number of multiplications. Compared to existing differentiator [18], the proposed fourteenth-order differentiator has higher stopband magnitude response

Table 2 $\omega_p = 0.5\pi$, $\omega_s = 0.725\pi$. Results of comparison of proposed differentiators with lowpass differentiator from [18].

Parameters	Proposed $L = m = 4$, $\gamma = 1.75$	Proposed $L = m = 4$ $\gamma = 2.875$	[18]
δ_p	1.31%	1.10%	3.79%
δ_s	8.44%	15.61%	36.3%
$\overline{\tau}$	2.73	2.37	2.45
η	7.22°	1.15°	1.21°
no. of multiplications	4	4	3
no. of delays/filter order	6	6	6

error only, while the proposed twelfth-order differentiator has considerable higher passband phase response linearity error and somewhat higher stopband magnitude response error.

Table 3 $\omega_p = 0.7\pi$, $\omega_s = 0.825\pi$. Results of comparison of proposed differentiators with lowpass differentiator from [18].

Parameters	Proposed $L = m = 6$, $\gamma = 2.25$	Proposed $L = m = 7$, $\gamma = 2.75$	Proposed $L = 10$, $m = 9$, $\gamma = 2.75$	[18]
δ_p	0.72%	0.40%	0.34%	0.84%
δ_s	15%	33.68%	5.06%	10.05%
$\overline{\tau}$	4.63	5.42	8.42	8.52
η	12.41°	3.48°	3.37°	4.61°
no. of multiplications	6	7	10	9
no. of delays/filter order	12	14	18	18

The results presented in examples 5, 6 and 7 lead to the conclusion that proposed differentiators compare favorably with existing allpass-based IIR lowpass differentiators [18] of the same order. On the other hand, due to the fact that maximum of the magnitude response of proposed lowpass differentiators equals γ, while higher values of parameter γ are required to obtain nearly-linear phase, existing allpass-based lowpass differentiators from [18] have lower maximum of the magnitude response.

4.2 Comparison with the nearly-linear phase lowpass differentiators from [12]

Comparison of the proposed lowpass differentiators with differentiators from [12] is presented in this subsection. These differentiators are designed by minimizing the group-delay deviation subject to constraints on maximum relative passband magnitude response error and average squared stopband magnitude response. Transfer function of lowpass differentiators from [12] can be expressed as

$$H_2(z) = \left(1 - z^{-1}\right) \frac{\sum_{i=0}^{M-1} q_i z^{-i}}{1 + \sum_{i=1}^{M} p_i z^{-i}}, \tag{40}$$

thus requiring $2M$ multiplications and M delays.

In the eighth example, proposed differentiators are compared to third-order lowpass differentiator from [12] with passband edge frequency $\omega_p = 0.3\pi$. Three differentiators are designed: a) $L = m = 3$, $\omega_s = 0.525\pi$, $\gamma = 1.25$, b) $L = m = 4$, $\omega_s = 0.45\pi$, $\gamma = 1.125$, and c) $L = 5$, $m = 4$, $\omega_s = 0.44\pi$, $\gamma = 1.5$. From the results presented in Table 4, it can be concluded that all differentiators designed using the proposed method outperform existing one in terms of δ_p, P_{sb}, and required number of multiplications. On the other hand, the proposed eighth-order differentiator has smaller phase response error, while the fourth- and sixth-order differentiators have somewhat higher value of passband phase response error compared to the existing differentiator from [12].

Table 4 $\omega_p = 0.3\pi$. Results of comparison of proposed differentiators with lowpass differentiator from [12].

Parameters	Proposed $L = m = 3$, $\omega_s = 0.525\pi$, $\gamma = 1.25$	Proposed $L = m = 4$, $\omega_s = 0.45\pi$, $\gamma = 1.125$	Proposed $L = 5$, $m = 4$, $\omega_s = 0.44\pi$, $\gamma = 1.5$	[12]
δ_p	3.05%	0.21%	0.86%	3.5%
P_{sb}	0.24	0.23	0.24	0.25
$\overline{\tau}$	1.94	3.06	3.73	3.36
η	4.96°	4.10°	1.50°	1.71°
no. of multiplications	3	4	5	6
no. of delays/filter order	4	6	8	3

In the ninth example, two differentiators having the same passband and stopband edge frequencies, $\omega_p = 0.5\pi$, $\omega_s = 0.63\pi$, are designed using the proposed method with following values: a) $L = m = 4$, $\gamma = 2.3125$, b) $L = 6$, $m = 5$, $\gamma = 2.5$. The results of comparison are presented in Table 5. From these results it can be concluded that tenth-order proposed lowpass differentiator outperform existing one in all terms except filter order and average group delay values. On the other hand, proposed sixth-order differentiator requires only four multiplications (compared to 6 multipliers required by the other proposed and existing differentiator), has lower values of δ_p and P_{sb}, but somewhat higher passband phase error (2.77°) compared to existing differentiator (1.74°).

In the tenth example, two tenth-order ($L = m = 6$) differentiators with passband edge frequency $\omega_p = 0.7\pi$ are designed using the proposed method: a) $\omega_s = 0.85\pi$, $\gamma = 2.25$, and b) $\omega_s = 0.815\pi$, $\gamma = 2.3125$, and compared to the lowpass differentiator from [12]. The results of comparison are summarized in Table 6, while magnitude response, relative passband magnitude response and phase linearity errors are given in Figure 8. Both proposed differentiators have higher group delay/filter order than existing one, while the first proposed differentiator has slightly higher passband phase error (12.2° compared to 11.96°).

The results presented in examples 7, 8 and 9 lead to the conclusion that the proposed allpass-based IIR lowpass differentiators, although of the higher order, require less multiplications compared to the existing lowpass differentiators from [12].

Table 5 $\omega_p = 0.5\pi$. Results of comparison of proposed differentiators with lowpass differentiator from [12].

Parameters	Proposed $L = m = 4$, $\omega_s = 0.63\pi$, $\gamma = 2.3125$	Proposed $L = 6$, $m = 5$, $\omega_s = 0.63\pi$, $\gamma = 2.5$	[12]
δ_p	1.98%	1.4%	6%
P_{sb}	0.87	0.76	0.88
$\overline{\tau}$	2.49	4.44	2.31
η	2.77°	1.7°	1.74°
no. of multiplications	4	6	6
no. of delays/filter order	6	10	3

Table 6 $\omega_p = 0.7\pi$. Results of comparison of proposed differentiators with lowpass differentiator from [12].

Parameters	Proposed $L = m = 6$, $\omega_s = 0.85\pi$, $\gamma = 2.25$	Proposed $L = m = 6$, $\omega_s = 0.815\pi$, $\gamma = 2.3125$	[12]
δ_p	0.61%	0.96%	1%
P_{sb}	1.18	1.2	1.2
$\overline{\tau}$	4.63	4.58	2.02
η	12.2°	9.69°	11.96°
no. of multiplications	6	6	8
no. of delays/filter order	10	10	4

4.3 Comparison with the nearly-linear phase lowpass differentiators from [5]

In this subsection, a comparison of the proposed nearly-linear phase IIR lowpass differentiators with the ones from [5] is presented. These differentiators are derived from the lowpass differentiators designed using cascading approach (second-order wideband differentiator [3] is cascaded with the third-order Chebyshev I lowpass filter with 0.1 dB passband ripple value) by altering the denominator coefficients such that magnitude and passband phase response linearity errors are simultaneously minimized. Transfer function of lowpass differentiators from [5] can be expressed as

$$H_3(z) = \frac{q_0\left(1 - z^{-2}\right)\left(1 + z^{-1}\right)^3}{1 + p_1 z^{-1} + p_2 z^{-2} + p_3 z^{-3} + p_4 z^{-4} + p_5 z^{-5}}, \tag{41}$$

thus requiring 6 multiplications and 5 delays.

In Examples 10, 11 and 12, proposed lowpass differentiators are compared to fifth-order differentiators from [5] with passband edge frequencies $\omega_p = 0.3\pi$, $\omega_p = 0.4\pi$ and $\omega_p = 0.5\pi$, respectively. The results of comparison are presented in Tables 7, 8 and 9. Magnitude responses, relative passband magnitude response errors and passband phase response linearity errors for $\omega_p = 0.4\pi$ are shown in Figure 9. From these results it can be concluded that the proposed fourth-order allpass-based IIR

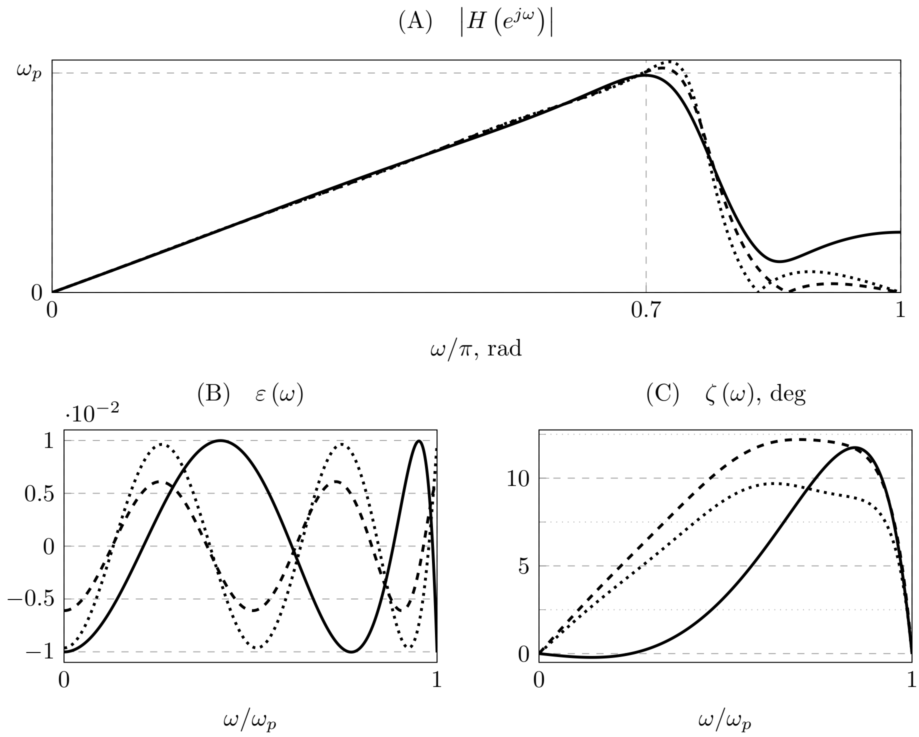

Fig. 8 $\omega_p = 0.7\pi$. (A) Magnitude responses, (B) relative passband magnitude response errors, and (C) passband phase response linearity errors of the IIR lowpass differentiator from [12] (solid line) and the proposed ones (dashed and dotted lines correspond to two tenth-order ($\gamma = 2.25$ and $\gamma = 2.1325$) differentiators, respectively).

lowpass differentiators have better or comparable performances than existing fifth-order differentiators from [5], while proposed sixth-order differentiators outperform fifth-order differentiators [5] in all terms except filter order and group delay values. Furthermore, proposed fourth- and sixth-order differentiators require significantly less multiplications compared to differentiators from [5].

Table 7 $\omega_p = 0.3\pi$. Results of comparison of proposed differentiators with lowpass differentiator from [5].

Parameters	Proposed $L = m = 3$, $\omega_s = 0.625\pi$, $\gamma = 1.125$	Proposed $L = m = 4$ $\omega_s = 0.55\pi$, $\gamma = 1.0625$	[5]
δ_p	2.04%	0.10%	2.56%
P_{sb}	0.23	0.22	0.24
$\overline{\tau}$	2.09	3.16	2.34
η	6.05°	5.38°	6.27°
no. of multiplications	3	4	6
no. of delays/filter order	4	6	5

Table 8 $\omega_p = 0.4\pi$. Results of comparison of proposed differentiators with lowpass differentiator from [5].

Parameters	Proposed $L = 3$, $m = 4$, $\gamma = 1.2745$	Proposed $L = m = 4$ $\omega_s = 0.6\pi$, $\gamma = 1.375$	[5]
δ_p	0.93%	0.39%	2.34%
P_{sb}	0.41	0.36	0.41
$\overline{\tau}$	2.08	2.92	1.98
η	10.94°	6.9°	10.58°
no. of multiplications	4	4	6
no. of delays/filter order	4	6	5

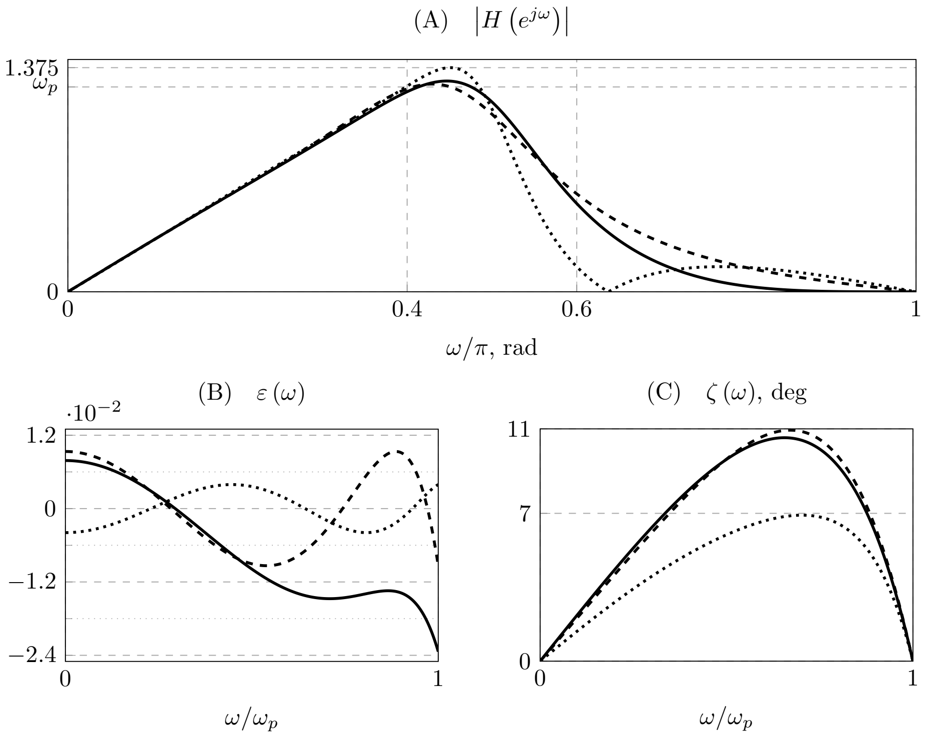

Fig. 9 $\omega_p = 0.4\pi$. (A) Magnitude responses, (B) relative passband magnitude response errors, and (C) passband phase response linearity errors of the IIR lowpass differentiator from [5] (solid line) and the proposed ones (dashed and dotted lines correspond to fourth- and sixth-order differentiators, respectively).

Table 9 $\omega_p = 0.5\pi$. Results of comparison of proposed differentiators with lowpass differentiator from [5].

Parameters	Proposed $L = 3$, $m = 4$, $\gamma = 1.584$	Proposed $L = m = 4$ $\omega_s = 0.7\pi$, $\gamma = 1.75$	[5]
δ_p	1.04%	1.46%	6.70%
P_{sb}	0.89	0.63	0.89
$\overline{\tau}$	1.88	2.73	1.66
η	11.54°	7.40°	11.77°
no. of multiplications	4	4	6
no. of delays/filter order	4	6	5

5 Conclusion

The paper presents the design of nearly-linear phase allpass-based IIR lowpass differentiators with the magnitude response approximating the ideal one in weighted Chebyshev sense both in the passband and the stopband. Employed parallel connection of two allpass filters whose orders differ by two, where allpass branch of lower order is a pure delay, allows formulation of the differentiator magnitude and phase responses as functions of the corresponding allpass filter phase response and maximum of the magnitude response (i.e. the value of the parameter γ). Relation between these two responses is such that the phase response linearity error can be effectively controlled by the maximum of the magnitude response and the maximum of the relative passband magnitude response error. This, if very low phase linearity errors (below few degrees) are required, leads to considerable magnitude response overshoot in the transition region. Therefore, instead of increasing the maximum of the magnitude response, phase correction of the proposed low-order lowpass differentiators may be a better solution. This will be a matter of future research.

Design examples demonstrate that even fourth-order differentiators (requiring only 3 or 4 multiplications depending on whether γ can be expressed as the sum of a few power-of-two terms or not) can have very low relative magnitude response errors and nearly-linear phases. Furthermore, proposed differentiators compare favorably with existing allpass-based IIR lowpass differentiators of the same order, while compared to other existing IIR nearly-linear phase lowpass differentiators, proposed differentiators require less multiplications.

Declarations

Funding

The authors received no financial support for the research.

Conflict of interest

The authors declare that they have no conflict of interest.

Data availability

Data sharing not applicable to this article as no datasets were generated or analysed during the current study.

Appendix A Allpass-based IIR lowpass differentiators design function

```
def designMethod(L, m, wp, ws, gamma):
    import sympy as sp
    import numpy as np
    import scipy.signal as scs

    def phi1(w): return int(w<=wp)*(-(L-2)*w - 2*sp.asin(w/gamma)) +\
        int(w>=ws)*(-(L-2)*w - 2*sp.pi)

    _a = sp.Matrix([1] + [sp.Symbol('a%d' % i, real=True)
                          for i in range(1, L+1)])
    _w = sp.Symbol('w', real=True)

    c = sp.Matrix([sp.cos(n*_w) for n in range(L+1)]).T
    s = sp.Matrix([sp.sin(n*_w) for n in range(L+1)]).T
    sc = sp.Matrix([(n-1)*sp.sinc(_w*(n-1)) for n in range(L+1)]).T

    _lmbd = (sc*_a)[0] / sp.sqrt((c*_a)[0]**2 + (s*_a)[0]**2)
    _grad_lmbd = [_lmbd.diff(_a[i]) for i in range(1, L+1)]

    # Step 1
    w = [(k+2)*wp/(m+2) for k in range(1, m)] + \
        [ws + (k-m+1)*(np.pi-ws)/(L-m+2) for k in range(m, L+1)]

    B = sp.Matrix([[sp.sin((phi1(w[k]) + (L - 2*i)*w[k]) / 2)
                    for i in range(1, L+1)] for k in range(L)])

    c = sp.Matrix([-sp.sin((phi1(w[k]) + L*w[k]) / 2) for k in range(L)])
    ap = np.array(list(B**-1 * c))

    w = np.linspace(0, 1, 10001) * np.pi
    wpass, wstop = w[w<=wp], w[w>=ws]
    dtol = 1e-10
    while True:
        lmbd = _lmbd.subs([(_a[i], ap[i-1]) for i in range(1, L+1)])
        lmbd = sp.lambdify(_w, lmbd)
        grad_lmbd = [_grad_lmbd[k].subs(
            [(_a[i], ap[i-1]) for i in range(1, L+1)]) for k in range(L)]
        grad_lmbd = sp.lambdify(_w, grad_lmbd)

        # Step 2
```

```
    def err_pass(w): return -1 - gamma*lmbd(w)
    def err_stop(w): return -w*gamma*lmbd(w)

    ind, _ = scs.find_peaks(abs(err_pass(wpass)))
    w_hat = np.append(np.append(0, wpass[ind]), wp)
    # extremas of the same sign
    if len(w_hat)>m and \
        np.sign(err_pass(w_hat[0]))==np.sign(err_pass(w_hat[1])):
        w_hat = w_hat[1:]
    if len(w_hat)>m and \
        np.sign(err_pass(w_hat[-1]))==np.sign(err_pass(w_hat[-2])):
        w_hat = w_hat[:-1]
    # m+1 sign-alternating extrema
    if len(w_hat) > m:
        if wp >= np.pi/2:
            w_hat = w_hat[:-1]
        elif abs(err_pass(w_hat[0])) > abs(err_pass(w_hat[-1])):
            w_hat = w_hat[:-1]
        else:
            w_hat = w_hat[1:]
    p = int(np.sign(err_pass(w_hat[0])) == 1)

    ind, _ = scs.find_peaks(abs(err_stop(wstop)))
    w_ol = np.append(ws, wstop[ind])
    if len(w_ol) > (L-m+2):
        if abs(err_stop(ws)) > abs(err_stop(ws[-1])):
            w_ol = w_ol[:-1]
        else:
            w_ol = w_ol[1:]

    # Step 3
    Lhs = [[sp.Matrix([grad_lmbd(w_hat[k]) for k in range(m)]),
            sp.Matrix([(-1)**(p+k) for k in range(1, m+1)]),
            sp.zeros(m, 1)],
           [sp.Matrix([grad_lmbd(w_ol[k]) for k in range(L-m+2)]),
            sp.zeros(L-m+2, 1),
            sp.Matrix([(-1)**(k+1) / w_ol[k] for k in range(L-m+2)])]]
    Lhs = sp.Matrix(Lhs)
    rhs = sp.Matrix(-np.append(1/gamma + lmbd(w_hat), lmbd(w_ol)))
    x = Lhs**-1 * rhs
    a = ap + np.array(x[:L])

    if abs(np.array(x[:L])).max() <= dtol:
        break
    else:
        ap = a
return a
```

References

[1] Ababneh, J., Khodier, M.: Design of Approximately Linear Phase Low Pass IIR Digital Differentiator using Differential Evolution Optimization Algorithm, Circuits, Systems, and Signal Processing, 1–23 (2021)

[2] Al-Alaoui, M.A: Novel approach to designing digital differentiators, Electronics Letters **28**(15), 1376–1378 (1992)

[3] Al-Alaoui, M.A: Novel IIR differentiator from the Simpson integration rule, IEEE Transactions on Circuits and Systems I: Fundamental Theory and Applications **41**(2), 186–187 (1994)

[4] Al-Alaoui, M.A: A class of second-order integrators and low-pass differentiators, IEEE Transactions on Circuits and Systems I: Fundamental Theory and Applications **42**(4), 220–223 (1995)

[5] Al-Alaoui, M.A: Linear phase low-pass IIR digital differentiators, IEEE Transactions on signal processing 55(2), 697–706 (2007)

[6] Al-Alaoui, M.A.: Direct approach to image edge detection using differentiators, in 2010 17th IEEE International Conference on Electronics, Circuits and Systems, 154–157 (2010)

[7] Ferdi, Y.: Improved lowpass differentiator for physiological signal processing, in 2010 7th International Symposium on Communication Systems, Networks & Digital Signal Processing (CSNDSP 2010), 747–750 (2010).

[8] Goldberger, A.L., Amaral, L.A., Glass, L., Hausdorff, J.M, Ivanov, P.Ch., Mark, R.G, Mietus, J.E., Moody, G.B., Peng, C.-K., Stanley, H.E.: PhysioBank, PhysioToolkit, and PhysioNet: Components of a New Research Resource for Complex Physiological Signals, Circulation **101**(23), e215–e220 (2000)

[9] Krstić, I.: Design of IIR lowpass differentiators based on second-order allpass filter application, Circuits, Systems, and Signal Processing **41**(3), 1803–1818 (2022)

[10] Le Bihan, J.: Novel class of digital integrators and differentiators, Electronics Letters **29**(11), 971–973 (1993)

[11] Merino, M., Rivera, O., Gómez, I., Molina, A., Dorronzoro, E.: A Method of EOG Signal Processing to Detect the Directions of Eye Movements, in 2010 First International Conference on Sensor Device Technologies and Applications, July 2010, 100–105.

[12] Nongpiur, R.C., Shpak, D.J., Antoniou, A.: Design of IIR digital differentiators using constrained optimization. IEEE Trans. Signal Processing **62**(7), 1729–1739 (2014)

[13] Pan, J., Tompkins, W.J.: A real-time QRS detection algorithm, IEEE transactions on biomedical engineering (3), 230–236 (1985)

[14] Platas-Garza, M.A., Platas-Garza, J., Serna, J. A. de la O: Dynamic phasor and frequency estimates through maximally flat differentiators, IEEE Transactions on instrumentation and measurement **59**(7), 1803–1811 (2009)

[15] Regalia, P.A., Mitra, S.K., Vaidyanathan, P.: The digital all-pass filter: A versatile signal processing building block, Proceedings of the IEEE **76**(1), 19–37 (1988)

[16] Skogstad, S.A., Holm, S., Hivin, M.: Designing digital IIR low-pass differentiators with multi-objective optimization, in 2012 IEEE 11th International Conference on Signal Processing **1**, Oct 2012, 10–15.

[17] Stančić, G., Krstić, I., Živković, M: Design of IIR fullband differentiators using parallel all-pass structure, Digital Signal Processing **87**, 132 – 144 (2019)

[18] Stančić, G., Krstić, I., Cvetković, S.: All-pass-based design of nearly-linear phase IIR low-pass differentiators, International Journal of Electronics **107**(9), 1451–1470 (2020)

[19] Wulf, M., Staude, G., Knopp, A., Felderhoff, T.: Efficient design of FIR filter based low-pass differentiators for biomedical signal processing, Current Directions in Biomedical Engineering **2**(1), 215–219 (2016)

[20] Yi, H., Lai, X.: Design of low-pass and band-pass infinite impulse response maximally flat stable digital differentiators, IET Signal Processing, **16**(2), 201– 219 (2022)

[21] Yoshida, T., Nakamoto, M., Aikawa, N.: Low-delay and high-functioning digital differentiators in the big data era, Electronics and Communications in Japan **101**(10), 31–37 (2018)

[22] Yoshida, T.: Low-pass maximally flat IIR digital differentiator design with arbitrary flatness degree, in 2021 Asia-Pacific Signal and Information Processing Association Annual Summit and Conference (APSIPA ASC), 226–231 (2021)